ON THE CONCENTRATION GRADIENT ACROSS A SPHERICAL SOURCE WASHED BY SLOW FLOW

LIONEL JAFFE
From the Department of Biology, University of Pennsylvania, Philadelphia

ABSTRACT A model has been numerically analyzed to help interpret the orienting effects of flow upon cells. The model is a sphere steadily and uniformly emitting a diffusible stuff into a medium otherwise free of it and moving past with Stokes flow. Its properties depend primarily upon the Peclet number, *Pe*, equal to $a \cdot v_\infty/D$, *i.e.*, the sphere's radius, a, times the free stream speed, v_∞, over the stuff's diffusion constant, D. As *Pe* rises, and washing becomes more effective, the average surface concentration, $\bar{C}_{sa}$ falls (Figs. 2 and 5) and the residual material becomes relatively concentrated on the sphere's lee pole (Figs. 2 and 4). Specifically, as *Pe* rises from 0.1 to 1, the relative concentration gradient, G, rises from 0.7 to 5.0 per cent and to the point where it is rising at about 8 per cent per decade; by *Pe* 1000, $G = 22.1$ per cent. From *Pe* 1 through 1000, $G/(1 - \bar{C}_{sa})$, or the gradient per concentration deficiency remains at about 26 per cent suggesting that G approaches a ceiling of about 26 per cent. Also from *Pe* 1 through 1000, the average mass transfer coefficient nearly equals that previously calculated for spheres maintaining constant surface concentration instead of flux. The complete differential equation without approximations, the Gauss-Seidel method, and an approximation for the outer boundary condition were used.

INTRODUCTION

One way to explore the pattern of growth or movement controlling substances around a cell is to measure the orienting effects of flow. Thus, under slow flow, a spore of the fungus, *Botrytis* tends to germinate downstream; it does so because it emits a diffusible stimulator which persists on its lee side. In other words, each spore's growth tends to be oriented by a concentration gradient of a stuff which it emits uniformly but is redistributed by flow past it (1).

To help analyze such studies I have computed steady-state distributions of a diffusible stuff over the surface of a spherical source washed by Stokes flow, assuming a uniform normal flux over this "cell." Three general considerations guided these computations:

First, it follows from the Weber-Fechner law generally—and even from a little evidence of its applicability to cellular chemo-orientation specifically (2–3)—that

the degree of cell orientation will depend upon some measure of the *relative* concentration gradients across them. I would guess that a sufficient approximation to this unknown measure is "the gradient," G:

$$G = \int_0^\pi C_s \cdot \cos\theta \, d\theta \Big/ \int_0^\pi C_s \, d\theta \tag{1}$$

where C_s = concentration at a point on the cell's surface,

θ = latitude with respect to the flow axis, zero being upstream.

The gradient, then, is the primary desidiratum, and its accuracy a main guide to computation.

Secondly, it follows from simple analytical considerations that the distributions have the general form:

$$C_s = C_{s_0} \cdot \bar{C}_s(\theta, Pe) \tag{2}$$

where C_{s_0} = concentration on the cell's surface in a stagnant medium,

Pe = Peclet number (based on the radius), a dimensionless parameter equal to $a \cdot v_\infty / D$, where in turn,

v_∞ = flow speed far from the cell,

a = cell's radius,

D = stuff's diffusion constant.

Evidently then: $\bar{C}_s$ = a surface concentration under flow relative to that in a stagnant medium, and:

$$G = \int_0^\pi \bar{C}_s \cdot \cos\theta \, d\theta \Big/ \int_0^\pi \bar{C}_s \, d\theta. \tag{3}$$

That is, the gradient depends only upon the Peclet number.

Thirdly, it is of primary importance to obtain results for an intermediate range of Peclet numbers, perhaps 1 through 100, since for $Pe \ll 1$, flow will be too slow to effect a significant gradient while for $Pe \gg 100$, it will be so rapid as—in real experiments—to influence cells through a confusing mixture of mechanisms.

The large literature on transport from spheres under flow (4–10) is of relatively little use here since: (*a*) Sources maintaining a constant concentration (rather than constant flux) at their surfaces are considered, and/or (*b*) Only the flux averaged over the sphere's surface is calculated, and/or (*c*) Intermediate Peclet ranges are not considered, and/or (*d*) Low Reynolds numbers are not considered, *etc.* These limitations arise not only from different objectives—those of engineering—but also from the difficulty of obtaining solutions by analytical means. One thing made plain is the need for numerical analysis.

METHODS

In Brief The region analyzed is bounded by the spherical source and an outer concentric sphere. However, since the system is symmetrical about the flow axis, the

governing differential equation is two-dimensional and the region analyzed can be considered a semiannulus (Fig. 1). The inner boundary condition is one of constant normal flux; the outer, a crude estimate of the concentration, C. Using polar coordinates and central differences the differential equation was converted to a system of finite difference equations which were then solved by the Gauss-Seidel method with the aid of I.B.M. 7074 and 7094 computers. The results reported required the equivalent of about one and one-half hours of actual computation time on the 7094.

Differential Equation. The basic equation is well known. It develops from the idea that in the steady state in any small volume, the rate of concentration change due to diffusion (as described by Fick's law) is compensated by convection; the velocity field is given by the Stokes solution. (See reference 9, p. 388 or reference 4, p. 81.) This yields the following elliptic equation in polar coordinates:

$$(r^2)\partial^2 C/\partial r^2 + \partial^2 C/\partial \theta^2 + (2r - Pe \cdot v_r \cdot r^2)\partial C/\partial r + (\text{ctn } \theta - Pe \cdot v_\theta \cdot r)\partial C/\partial \theta = 0 \quad (4)$$

where v_r and v_θ are the normalized components of the velocity field, thus:

$$\begin{aligned} v_r &= -(1 - 1.5r^{-1} + 0.5r^{-3}) \cos \theta \\ v_\theta &= (1 - 0.75r^{-1} + 0.25r^{-3}) \sin \theta \end{aligned} \quad (5)$$

Boundary Conditions. The system is conveniently normalized by setting,

$$a = 1 \qquad D = 1 \qquad P = 4\pi \quad (6)$$

where P is the total rate of production of the stuff. Hence, too, $C_{s0} = 1$, and $C_s = \bar{C}_s$. C_R, the concentration on the outer boundary is crudely approximated as follows (Fig. 1):

$$\begin{aligned} C_R &= 0 && \text{for } \theta \leq \pi/2 \\ C_R &= K && \text{for } \theta \geq \bar{\theta} \\ C_R &= K\left(\frac{\theta - \pi/2}{\bar{\theta} - \pi/2}\right) && \text{for } \pi/2 < \theta < \bar{\theta} \end{aligned} \quad (7)$$

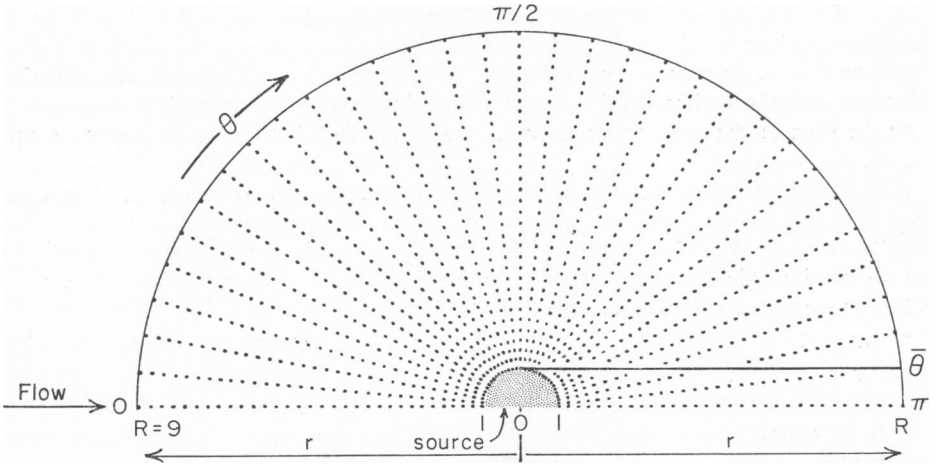

FIGURE 1 Illustration of the region analyzed. This is the region for Pe 1 with the finest grid used (32 × 32).

TABLE I

RADII OF THE OUTER BOUNDARIES USED IN THE ANALYSES

Note that the inner, source sphere's radius was set at unity (Fig. 1).

Pe	0.1	0.2	0.5	1	3	10	100	1000
R	25	17	13	9	6	3.7	1.8	1.3

where $\bar{\theta} = \pi/2 + \cos^{-1}(R^{-1})$

$R =$ outer boundary's radius.

Then K is calculated to make the total convective flux across the outer boundary equal to P. This procedure yields:

$$K = 4/Pe(R^2 - 1.5R + 0.5R^{-1})(\cos^2 \bar{\theta} + 0.25\bar{\theta}^{-1} \sin 2\bar{\theta} - 0.5 \cos 2\bar{\theta}) \quad (8)$$

Values of R large enough to sufficiently reduce the error thus introduced into the concentrations on the source's surface, C_s, were selected by exploring C_s as a function of R for each value of Pe used. (Table I.) Costs of these preliminary computations were minimized by using relatively coarse grids and by first estimating the required R value on the basis of the theoretical error function:

$$E = e^{-Pe(R-1.5 \ln R-0.25R^{-2}-0.75)} \quad (9)$$

The clearest derivation of E starts by considering the downstream region near $\theta = \pi$ where tangential transport is negligible. Within a small solid angle there, the differential equation takes the simple form:

$$-D \cdot dC/dr \cdot r^2 + v_r \cdot C \cdot r^2 = \text{constant radial flux.} \quad (10)$$

One can then easily obtain C_s and show that:

$$\partial C_s/\partial C_r = E. \quad (11)$$

The Course of Solution. The differential equation was reduced to finite differences equations involving Δr and $\Delta\theta$. This was routine except for a small trick where $\theta = 0$ or $\theta = \pi$. Here $ctn\theta$ goes to infinity, but this troublesome term cancels out of the difference equations when explicit use is made of the symmetry around the flow axis.

At the start of the iterative procedure, all recalculated C values were simply set equal to zero.

With $Pe \leq 100$, and beyond a relatively small number of sweeps, C_s always rose steadily during the iteration process and converged upon values that rose steadily from front to rear pole. For $Pe = 1000$, while certain combinations of increment sizes in the r and θ directions yielded gross instability, others sufficed to yield a reliable solution.

The convergence criterion depended on

$$\omega = 1 - (C_{sf})_{i-N_R}/(C_{sf})_i \quad (12)$$

where $(C_{sf})_i$ is the value of C at the source's rear pole after i iterations and N_r is the number of nodes in the radial direction (N_r was generally about 20). I used C_{sf} since it was seen to converge most slowly. Generally, computation was stopped when ω fell below 10^{-2}, though spot checks were extended to 10^{-3}.

Let N_r and N_θ represent the number of nodes in the radial and tangential directions,

TABLE II

METHOD OF EXTRAPOLATING TO THE VALUE OF THE GRADIENT, G (LEFT) OR OF THE AVERAGE CONCENTRATION, $\bar{C}_{sA}$ (RIGHT) FOR AN INFINITELY FINE MESH

These results are for Pe 1. The figures in the body of the table are values of G (in per cent terms) or $\bar{C}_{sa}$ as computed for the indicated finite meshes.

N_θ:	6	8	16	32	∞	6	8	16	32	∞
N_r										
16	6.3	5.6	4.9	4.7		0.606	0.604	0.602	0.602	
32	6.6			5.0		0.758			0.753	
64	6.7					0.796				
∞					5.0 ± 0.1					0.80 ± 0.01

respectively. Then for each Peclet number, the grid selection procedure was to compute the C_s curve, and then G with a pair of small values for N_r and N_θ (*i.e.* a very coarse grid), recompute with N_θ fixed at the first low value and N_r increasing and then *vice versa*, inspect the gradients so obtained, then, if appropriate, make a final computation with high values of N_r and N_θ, and finally extrapolate to the gradient for an infinitely fine grid. This process is illustrated by the results for $Pe = 1$ shown in Table II (left). Besides the gradient, it was also of some interest to compute the average surface concentration, $\bar{C}_{sa}$ from the same C_s curves. The results for $Pe = 1$ are shown in Table II (right). Note that the gradient required a relatively fine grid tangentially for enough accuracy while the average required a finer grid radially. Since the computational requirements for G and for $\bar{C}_{sa}$ differed thusly, and since G was the first objective, somewhat more extensive and accurate data are reported for G than for C_{sa} in the main results section.

The finest grids used generally had about a thousand nodes and took about 300 to 2000 sweeps to converge. The computation at each of the $N_r \times N_\theta$ nodes at which C was recalculated during each sweep took about 110 microseconds on the 7094 machine.

Errors. The results made it obvious that the largest errors generally arose from the finite number of nodes. These so called discretation errors were estimated by inspection of tables such as Table II and are the main components of the estimated over-all computational errors.

RESULTS AND DISCUSSION

The computer's raw output consists of concentrations (relative to those in a stagnant medium) at each node of the region analyzed; however, I report only surface concentrations, represented by $\bar{C}_s$, since these are most reliable and applicable. Data computed with the finest grids used are shown in Fig. 2.

Evidently, the $\bar{C}_s$ functions of θ are bell-shaped curves peaking at the sphere's rear pole. Over the range graphed, the main-and expected-change of these curves as the Peclet number rises and washing becomes more effective is simply a fall in the average concentration. It is also seen that the curves peak somewhat more sharply as Pe rises.

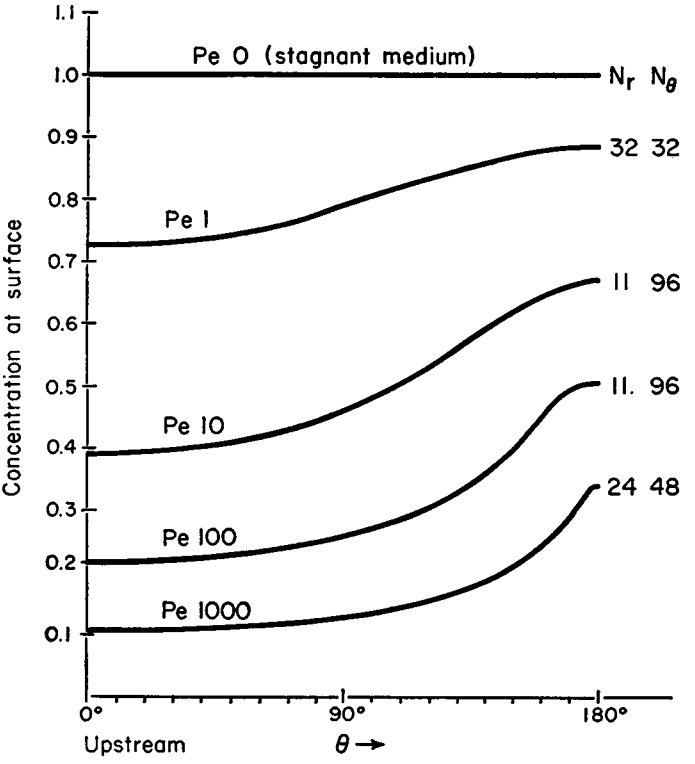

FIGURE 2 Concentrations at the source sphere's surface relative to that in a stagnant medium for various Peclet numbers. The number of nodes in the grids used to compute these results are shown at the right. These are raw data except at *Pe* 1 where a small correction for the discretation error was applied (all computed values were increased by 7 per cent).

TABLE III

PARAMETERS CHARACTERIZING CONCENTRATIONS AT SURFACE OF SPHERE UNDER SLOW FLOW (SEE TEXT)

Pe	*G*	$\bar{C}_{sa}$	$1/F$	$G/(1-\bar{C}_{sa})$
0	0			
0.1	0.7 ± 0.1			
0.2	1.3 ± 0.1			
0.5	3.0 ± 0.1	0.91 ± 0.05	0.86	
1	5.0 ± 0.1	0.80 ± 0.01	0.81	25 ± 1
3	8.9 ± 0.1	0.67 ± 0.01	0.68	27 ± 1
10	12.8 ± 0.1	0.53 ± 0.005	0.54	27.3 ± 0.4
100	18.7 ± 0.2	0.297 ± 0.002	0.306	26.6 ± 0.4
1000	22.1 ± 0.3	0.153 ± 0.001	0.159	26.1 ± 0.4
∞	26 ?	0	0	26 ?

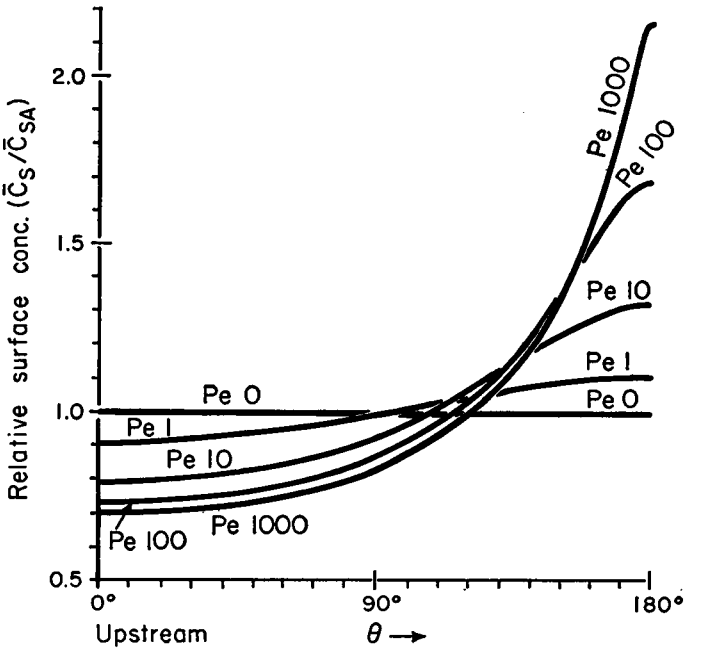

FIGURE 3 Concentrations at the source sphere's surface relative to the average surface concentration at each Peclet number.

The immediate application seems to involve a response to the relative concentration distributions across cells, that is the ratios $\bar{C}_s/\bar{C}_{ss}$ where $\bar{C}_{ss}$ is the concentration averaged over the surface. Starting with the data of Fig. 2, these are plotted in Fig. 3. They are again a family of bell-shaped curves peaking with increasing sharpness at the downstream pole as *Pe* rises.

My measures, *G*, of the relative concentration gradients across the sphere (as defined in equation (1) and as calculated from $\bar{C}_s$ curves and extrapolated to infinitely fine grids) are reported, in per cent terms, in Fig. 4 and Table III. As might be expected

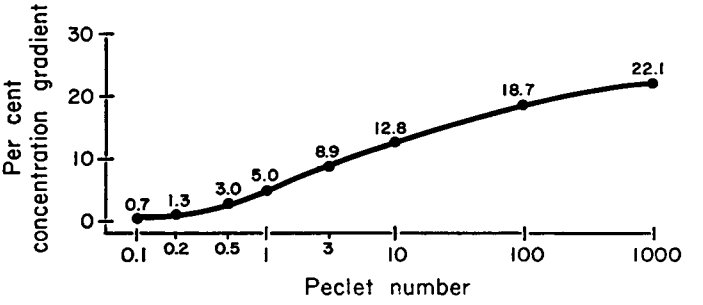

FIGURE 4 *G*, the relative concentration gradient across the sphere (in per cent terms) as a function of the Peclet number.

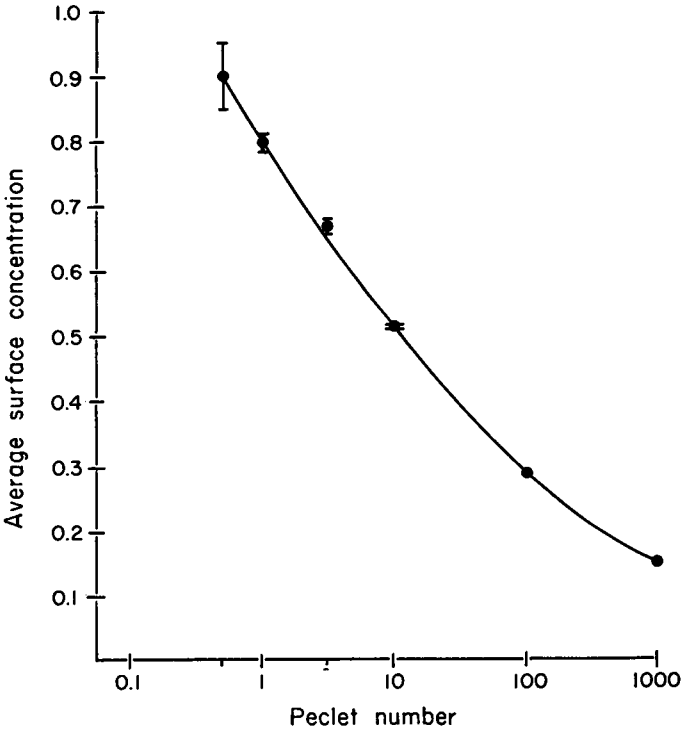

FIGURE 5 The average concentration at the sphere's surface relative to that in a stagnant medium for various Peclet numbers.

on dimensional grounds, G rises most swiftly near Peclet one. It rises about sevenfold, from 0.7 to 5.0 per cent, and to a point where it is rising at about 8 per cent per decade, as Pe rises from 0.1 to 1. However, even at Pe 1000, G only reaches 22 per cent.

The average surface concentrations (relative to those in a stagnant medium), $\overline{C}_{s,a}$, are shown in Fig. 5 and Table III. Also in this table I have listed the function $G/(1 - C_{s,a})$, or gradient per concentration deficiency. It is remarkably constant, at about 26 per cent, for Peclet numbers from 1 to 1000. Since the concentration must go to zero as Pe rises, this would suggest a limiting value of 26 per cent for the gradient at high Pe.

Using somewhat cruder methods, various investigators (5–8) have computed the average surface *fluxes* for spheres maintaining a constant surface concentration under Stokes flow. The most accurate data seems to be that of Ward (6). Again in Table III, I have listed the reciprocals, $1/F$ of Ward's flux values (relative to the stagnant case). At least from Pe 1 through 1000, the average surface concentration at constant flux is evidently close or perhaps even equal to the average reciprocal flux at constant concentration. In other words, the so called mass transfer coefficients, or fluxes per concentration difference are similar or the same for the two extreme

boundary conditions. It would certainly be interesting to get some understanding of this curious fact as well as of the above noted constancy of $G/(1 - C_{s\infty})$.

All these results hold for a cell emitting a stuff into a medium otherwise free of this material. If the flowing medium bears the background concentration, C_b, then it follows from the independence of diffusing particles and equation (2) that

$$C_s = C_{s\infty} \cdot \bar{C}_s + C_b \tag{12}$$

Solution of an elementary differential equation yields:

$$C_{s\infty} = P/4\pi a D \tag{13}$$

where P is the total rate of emission of the stuff.
Hence:

$$C_s = (P/4\pi a D) \cdot \bar{C}_s + C_b \tag{14}$$

The gradient thus produced will approach zero at *any* Peclet number as the background concentration rises.

Now, there is nothing in the derivation which depends upon P being positive. If P is negative, that is if the cell is *absorbing* the stuff at the rate P, then equation (11) is still valid as long as $C_s \geq 0$. For a cellular sink, then, the concentration is lowest rather than highest on the lee side, and the gradient will become very high at *any* positive Peclet number when P, $\bar{C}_s(Pe)$, and C_b are such that the concentration at the rear pole approaches zero. On the other hand, just as with a source, if C_b is high enough the gradient will approach zero. So P, and C_b must be known, as well as Pe to calculate flow gradients across an absorber. Furthermore, the equal flux assumption, while widely plausible for an emitter is likely to be of narrow validity for an absorbing cell. Altogether, then, such flow analysis is far more likely to be practically applicable to emitting than to absorbing cells.

This work was supported by both the National Science Foundation and the National Institutes of Health.

Received for publication, May 18, 1964.

REFERENCES

1. MÜLLER, D., and JAFFE, L., A quantitative study of cellular rheotropism, *Biophysic. J.*, 1965, **5**, in press.
2. BROKAW, C. J., Chemotaxis of bracken spermatozoids, *J. Exp. Biol.*, 1958, **35**, 197.
3. MIYOSHI, M., Ueber Chemotropismus der Pilze, *Botanische Zeitung*, 1894, **52**, 1.
4. LEVICH, V. G., Physiochemical Hydrodynamics, Englewood Cliffs, New Jersey, Prentice-Hall, Inc., 1962.
5. YUGE, T., Theory of heat transfer of spheres in uniform stream at low Reynolds numbers, Rep. 57, Institute of High Speed Mechanics, Tōhoku University, Sendai, Japan, 1955.
6. WARD, D. M., Mass transfer from solid and fluid spheres at low Reynolds numbers, Ph.D. Thesis, University of Toronto, 1961.
7. BOWMAN, C. W., WARD, D. M., JOHNSON, A. I., and TRASS, O., Mass transfer from fluid and solid spheres at low Reynolds numbers, *Canad. J. Chem. Eng.*, 1961, **39**, 9.

8. FRIEDLANDER, S. K., A note on transport to spheres in Stokes flow, *Am. Inst. Chem. Eng. J.*, 1961, **7**, 347.
9. ACRIVOS, A., and TAYLOR, T. D., Heat and mass transfer from single spheres in Stokes flow, *Physics. Fluids*, 1962, **5**, 387.
10. BROWN, W. S., PITTS, C. C., and LEPPERT, G., Forced convection heat transfer from a uniformly heated sphere, *J. Heat Transfer*, 1962, **84**, 133.